Bystander responses impact accurate detection of murine and human antigen-specific CD8+ T cells

Matthew D. Martin,[1] Isaac J. Jensen,[2] Andrew S. Ishizuka,[3] Mitchell Lefebvre,[2] Qiang Shan,[4] Hai-Hui Xue,[2,4,5] John T. Harty,[1,2,4] Robert A. Seder,[3] and Vladimir P. Badovinac[1,2,4]

[1]Department of Pathology and [2]Interdisciplinary Graduate Program in Immunology, University of Iowa, Iowa City, Iowa, USA. [3]Vaccine Research Center, National Institute of Allergy and Infectious Diseases, NIH, Bethesda, Maryland, USA. [4]Department of Microbiology and Immunology, University of Iowa, Iowa City, Iowa, USA. [5]Iowa City Veterans Affairs Health Care System, Iowa City, Iowa, USA.

Induction of memory CD8+ T cells is important for controlling infections such as malaria and HIV/AIDS and for cancer immunotherapy. Accurate assessment of antigen-specific (Ag-specific) CD8+ T cells is critical for vaccine optimization and for defining correlates of protection. However, conditions for determining Ag-specific CD8+ T cell responses ex vivo using intracellular cytokine staining (ICS) may be variable, especially in humans with complex antigens. Here, we used an attenuated whole parasite malaria vaccine model in humans and various experimental infections in mice to show that the duration of antigenic stimulation and timing of brefeldin A (BFA) addition influence the magnitude of Ag-specific and bystander T cell responses. Indeed, after immunization with an attenuated whole sporozoite malaria vaccine in humans, significantly higher numbers of IFN-γ–producing memory CD8+ T cells comprising Ag-specific and bystander responses were detected when the duration of Ag stimulation prior to addition of BFA was increased. Mechanistic analyses of virus-specific CD8+ T cells in mice revealed that the increase in IFN-γ–producing CD8+ T cells was due to bystander activation of Ag-experienced memory CD8+ T cells, and correlated with the proportion of Ag-experienced CD8+ T cells in the stimulated populations. Incubation with anti-cytokine antibodies (e.g., IL-12) improved accuracy in detecting bona fide memory CD8+ T cell responses, suggesting this as the mechanism for the bystander activation. These data have important implications for accurate assessment of immune responses generated by vaccines intended to elicit protective memory CD8+ T cells.

Introduction

CD8+ T cells have a role in mediating protection in humans against diverse pathogens impacting public health, such as HIV, influenza, and *Plasmodium*, the causative agent of malaria, and tumors (1–5). The critical factors for mediating protective immunity by T cells include the magnitude, quality, breadth, and location. Indeed, subjects with greater numbers of memory CD8+ T cells are better protected against infection (6, 7). Therefore, the development of preventive and therapeutic vaccines against infections and tumors requires a precise understanding of how to generate and accurately assess CD8+ T cell responses.

There are now a variety of techniques to measure CD8+ T cell responses, each with strengths and weaknesses. Peptide-MHC tetramer staining allows for an accurate enumeration of epitope-specific cells within the host and the evaluation of their phenotypic traits, but provides limited information on the functionality of the T cell response. Additionally, peptide-MHC tetramer analyses require knowledge of both the exact T cell epitope and MHC allele, which vary considerably between individuals, making assessment of the antigenic breadth of response resource-intensive. Antigen-stimulated detection of T cells by ICS, in contrast, allows for assessment of T cell responses in an MHC-agnostic manner, since stimulation of T cells occurs through autologous antigen (Ag) presentation. However, a limitation of the intracellular cytokine staining (ICS) assay, in which overlapping peptides are often used to stimulate T cells, is that the exact T cell epitope is not determined, and thus, the breadth of the host responses is not as precisely defined. Additionally, while ICS assays can provide data on the functional and phenotypic traits of responding cells, cells typically require stimulation for greater than 6 hours, during which time the cell phenotype of activated cells may change.

While alternative methods for detecting Ag-specific cells are used by some groups, such as activation-induced expression of CD137 (8), IFN-γ is the canonical gold-standard cytokine for ICS-based enumeration of Ag-specific CD8+ T cells. In a review of the literature, we determined that methods of conducting ICS, including length of incubation and timing of addition of brefeldin A (BFA; a Golgi-disrupting compound used to prevent secretion of cytokines), vary widely. Most often, ICS stimulation occurs for between 5 and 24 hours, and BFA is added several hours after the beginning of stimulation (4, 6, 9–39). While delaying addition of BFA may be necessary with certain types of Ag stimulation, such as use of whole pathogens rather than peptides to allow for Ag processing and presentation on MHC needed to drive cytokine production by CD8+ T cells, delayed BFA addition may also allow for the release of cytokines into the culture media when stimuli that have innate stimulatory activity are used. Inflammatory cytokines such as IL-12 could enhance IFN-γ production by Ag-specific CD8+ T cells that respond to antigens used for stimulation, but also by memory T cells that are specific for other antigens (bystander activation). This is supported by evidence that Ag-experienced effec-

Conflict of interest: The authors have declared that no conflict of interest exists.

Submitted: August 23, 2018; **Accepted:** June 18, 2019; **Published:** August 19, 2019.
Reference information: *J Clin Invest*. 2019;129(9):3894–3908.
https://doi.org/10.1172/JCI124443.

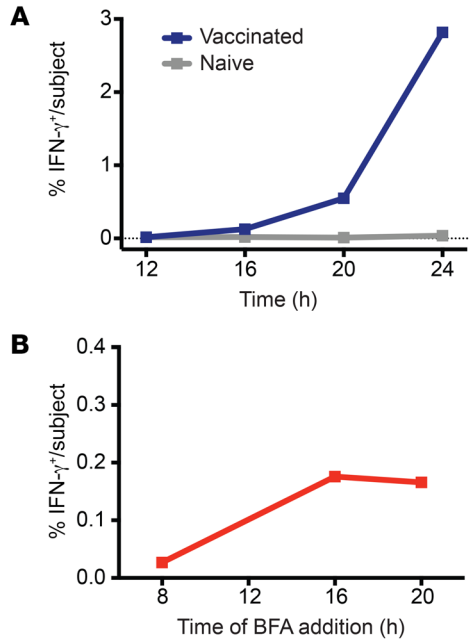

Figure 1. Increased length of incubation and delayed addition of BFA lead to elevated detection of IFN-γ–producing human CD8⁺ T cells following PfSPZ stimulation. (**A**) Percentage of CD8⁺ T cells producing IFN-γ when PBMCs from a PfSPZ-vaccinated or unvaccinated (naive) subject were stimulated with PfSPZs for 12, 16, 20, or 24 hours. (**B**) Percentage of CD8⁺ T cells producing IFN-γ when PBMCs from a PfSPZ-vaccinated subject were stimulated with PfSPZs for a total of 24 hours with BFA addition occurring after the first 8, 16, or 20 hours. *n* = 1.

tor or memory CD8⁺ T cells can be induced to produce IFN-γ not only in response to cognate Ag, but also in a bystander manner that is solely driven by inflammatory cytokines (40–42). Thus, we sought to understand how variations in the conditions of ICS impact the accurate accounting of infection- or vaccine-induced Ag-specific CD8⁺ T cells. These data have implications for improving vaccine design and accurately assessing correlates of CD8⁺ T cell–mediated protection.

Results

The frequency of IFN-γ–producing CD8⁺ T cells detected in humans following vaccination is increased with increased time of ex vivo Ag stimulation. The potency and protective capacity of a vaccine can be evaluated partly based on the magnitude of the induced memory CD8⁺ T cell population. To begin to address the impact of varying the assay conditions on enumeration of Ag-specific CD8⁺ T cell memory, we assessed the frequency of Ag-specific memory CD8⁺ T cells following vaccination of human subjects with an attenuated whole sporozoite malaria vaccine (4, 6, 43). Using a peptide stimulation assay for this vaccine would be technically challenging because of MHC polymorphism and the large number (>2000) of potential antigens presented to the immune system. Therefore, we used a previously developed assay in which stimulation of CD8⁺ T cells was achieved by incubation of PBMCs from vaccinated subjects with the vaccine itself, which consists of aseptic, purified, irradiated, metabolically active *Plasmodium falciparum* sporozoites (PfSPZs), and in which 12-hour stimulation was more sensitive than 6-hour stimulation (4). Here, we extended these data and incubated PBMCs from a vaccinated or nonimmunized subject with PfSPZs for 12, 16, 20, and 24 hours, adding BFA for the final 4 hours. While the nonimmunized subject had no IFN-γ production above background for the duration of stimulation, the percentage of CD8⁺ T cells that produced IFN-γ in the PfSPZ-vaccinated subject increased substantially over time (Figure 1A), suggesting that duration of ICS increased the detection of total IFN-γ–producing CD8⁺ T cells.

Addition of BFA is used in ICS assays to block release of IFN-γ within the T cell, thereby improving the sensitivity of the response. However, BFA also could inhibit efficient Ag processing and presentation of PfSPZs (44). To determine whether timing of BFA addition impacted the detection of IFN-γ–producing CD8⁺ T cells, cells were stimulated with PfSPZs for a total of 24 hours, with BFA being added after the first 8, 16, or 20 hours of incubation. A substantially higher percentage of CD8⁺ T cells producing IFN-γ was detected when BFA was added 16 or 20 hours after the beginning of stimulation (Figure 1B), indicating that the timing of BFA addition strongly influences the frequency of IFN-γ–producing CD8⁺ T cells detected.

Delayed addition of BFA would allow for soluble factors including inflammatory cytokines to be released into the culture, and potential bystander activation of Ag-experienced effector and memory CD8⁺ T cells. Thus, it is unclear whether enhanced detection of IFN-γ–producing CD8⁺ T cells following an increase in incubation time or a delay in addition of BFA was due to increased sensitivity of detection of *Plasmodium*-specific CD8⁺ T cells, and/or to triggering of IFN-γ production by nonmalaria Ag-experienced CD8⁺ T cells.

Delayed addition of BFA leads to bystander activation of Ag-experienced CD8⁺ T cells. To further determine how ICS conditions altered detection of Ag-specific CD8⁺ T cells, we used a well-defined mouse model that allows precise detection of CD8⁺ T cells of known Ag specificity. Mice (C57BL/6, Thy1.2) received adoptive transfer of naive T cell receptor–transgenic (TCR-transgenic) GP_{33}-specific P14 cells (Thy1.1) before LCMV-Armstrong infection (Figure 2A), and memory P14 cells were detected by Thy1.1 expression. Additionally, infection of C57BL/6 mice with LCMV elicits large Ag-specific CD8⁺ T cell responses that recognize LCMV-derived GP_{33} and NP_{396} epitopes (45), and we used peptide-stimulated ICS to detect cytokine-producing memory CD8⁺ T cells responding to GP_{33} and NP_{396} peptides (Figure 2, B–D). Mice generated in this manner contain endogenous (Thy1.1⁻, blue gates) CD8⁺ T cells comprising naive cells and Ag-specific cells that recognize GP_{33} and NP_{396} epitopes as well as additional LCMV-derived epitopes, and Ag-experienced P14 cells (Thy1.1⁺, red gates) that recognize GP_{33} but not NP_{396} peptides. Addition of P14 cells allows for detection of true Ag-specific responses (in response to GP_{33} peptide) and bystander responses (in response to NP_{396} peptide), while IFN-γ production by endogenous CD8⁺ T cells, owing to mixed epitope specificities of this population, could represent either true Ag-specific responses or responses that include both Ag-specific and bystander responses. To highlight this, as can be seen in Figure 2, B–D, we present detection of IFN-γ–producing cells following ICS gated on total lymphocytes (lymphocyte gate), total CD8⁺ T cells with identification of endogenous (blue gates) or P14 (red gates) cells based on Thy1.1 expression (CD8 gate), or total P14 cells [Thy1.1⁺CD8⁺ (P14) gate].

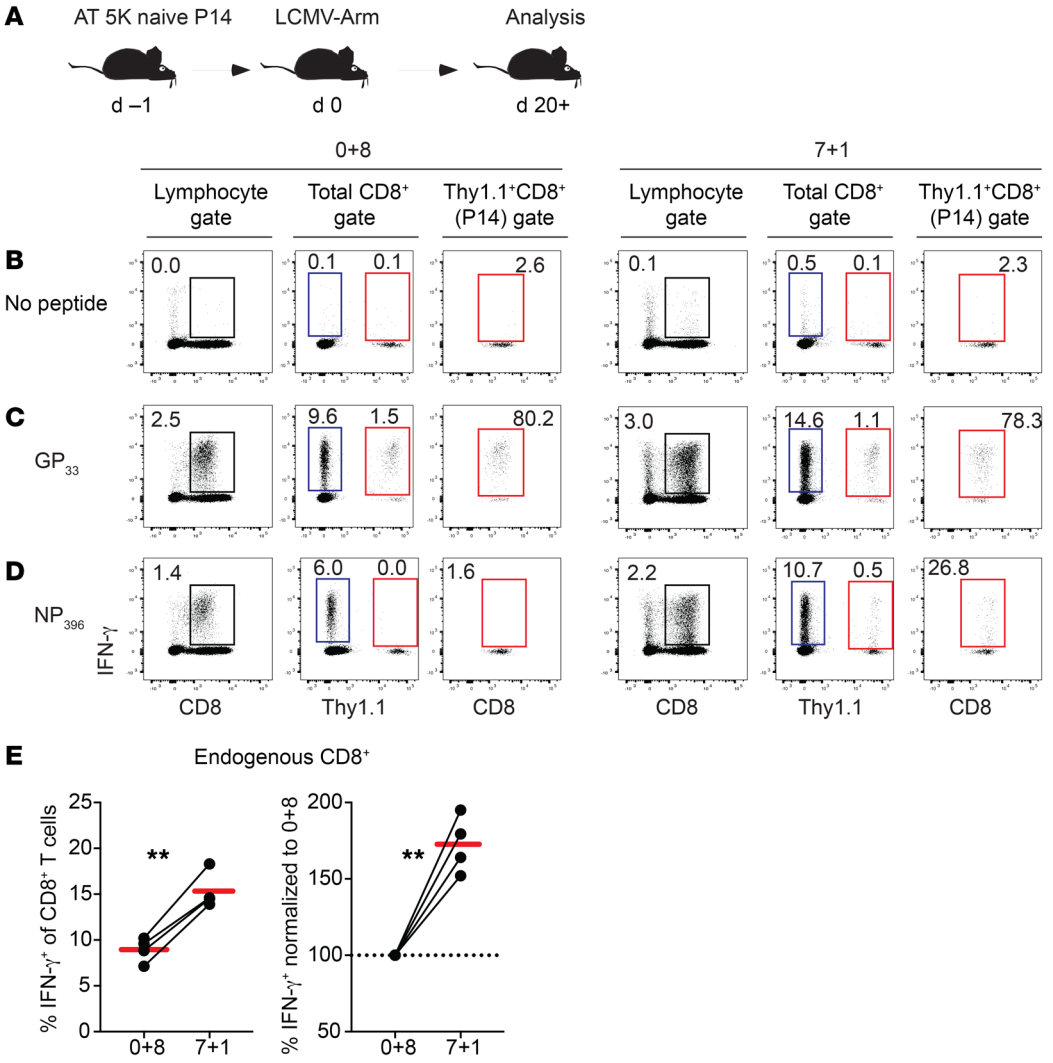

Figure 2. Delayed addition of BFA leads to bystander activation of CD8⁺ T cells. (**A**) Experimental design. Mice received adoptive transfer (AT) of naive P14 cells and were infected with LCMV-Armstrong. Approximately 3 weeks after infection, splenocytes were harvested and ICS was conducted. (**B**) Representative dot plots of IFN-γ production following 8-hour incubation without peptide and with BFA present for the entire incubation (0+8) or the final hour (7+1). Plots on the left are gated lymphocytes, plots in the middle are gated CD8⁺ T cells (Thy1.1⁻ = endogenous CD8⁺ T cells, Thy1.1⁺ = P14 cells), and plots on the right are gated P14 cells. Numbers inside plots indicate the percentage of cells producing IFN-γ out of all gated cells. (**C**) Representative dot plots of IFN-γ production following 8-hour incubation with GP_{33} peptide. (**D**) Representative dot plots of IFN-γ production following 8-hour incubation with NP_{396} peptide. (**E**) Left: Summary graphs of the percentage of endogenous CD8⁺ T cells producing IFN-γ following stimulation with GP_{33} peptide out of all CD8⁺ T cells with BFA present for the entire incubation (0+8) or the final hour (7+1). Right: Percentage of endogenous CD8⁺ T cells producing IFN-γ when BFA was added for the final hour of incubation normalized to the percentage when BFA was present for the entire incubation (dotted line, 100%). Representative data from more than 3 independent experiments. $n = 4$. Dots indicate individual mice. Solid red lines indicate the mean. $^{**}P < 0.01$ as determined by paired Student's t test.

Notably, since detection of IFN-γ–producing CD8⁺ T cells is impacted by peptide concentration and number of cells plated, we first identified conditions that allow for maximal detection of bona fide Ag-specific CD8⁺ T cells (2×10^6 cells per well and 200 nm peptide concentration) (Supplemental Figure 1, A and B; supplemental material available online with this article; https://doi.org/10.1172/JCI124443DS1). Inflammatory cytokines can potentially cause bystander activation of Ag-experienced CD8⁺ T cells when BFA is not present during the entire incubation (40–42, 46), so we first sought to determine whether timing of BFA addition impacted detection of IFN-γ–producing CD8⁺ T cells following specific peptide stimulation. Interestingly, an approximately 1.5- to 2-fold increase in the percentage of endogenous CD8⁺ T cells producing IFN-γ in response to GP_{33} or NP_{396} peptide was observed when BFA was added for the last hour (7+1) compared with when it was present during the entire incubation (0+8) (Figure 2, B–D, CD8 gate, blue boxes; and Figure 2E). Similar results were observed for LCMV-immune mice that did not receive P14 cells (Supplemental Figure 1, C and D).

A similar percentage of P14 cells produced IFN-γ following GP_{33} peptide stimulation regardless of timing of BFA addition (Figure 2C, P14 gate), suggesting that delayed addition of BFA does not impact IFN-γ production of bona fide Ag-specific CD8⁺ T cells. To determine whether increases in IFN-γ–producing CD8⁺ T cells that occurred with delayed BFA addition were due to bystander activation, we examined responses of "sensor" GP_{33}-specific Thy1.1 P14

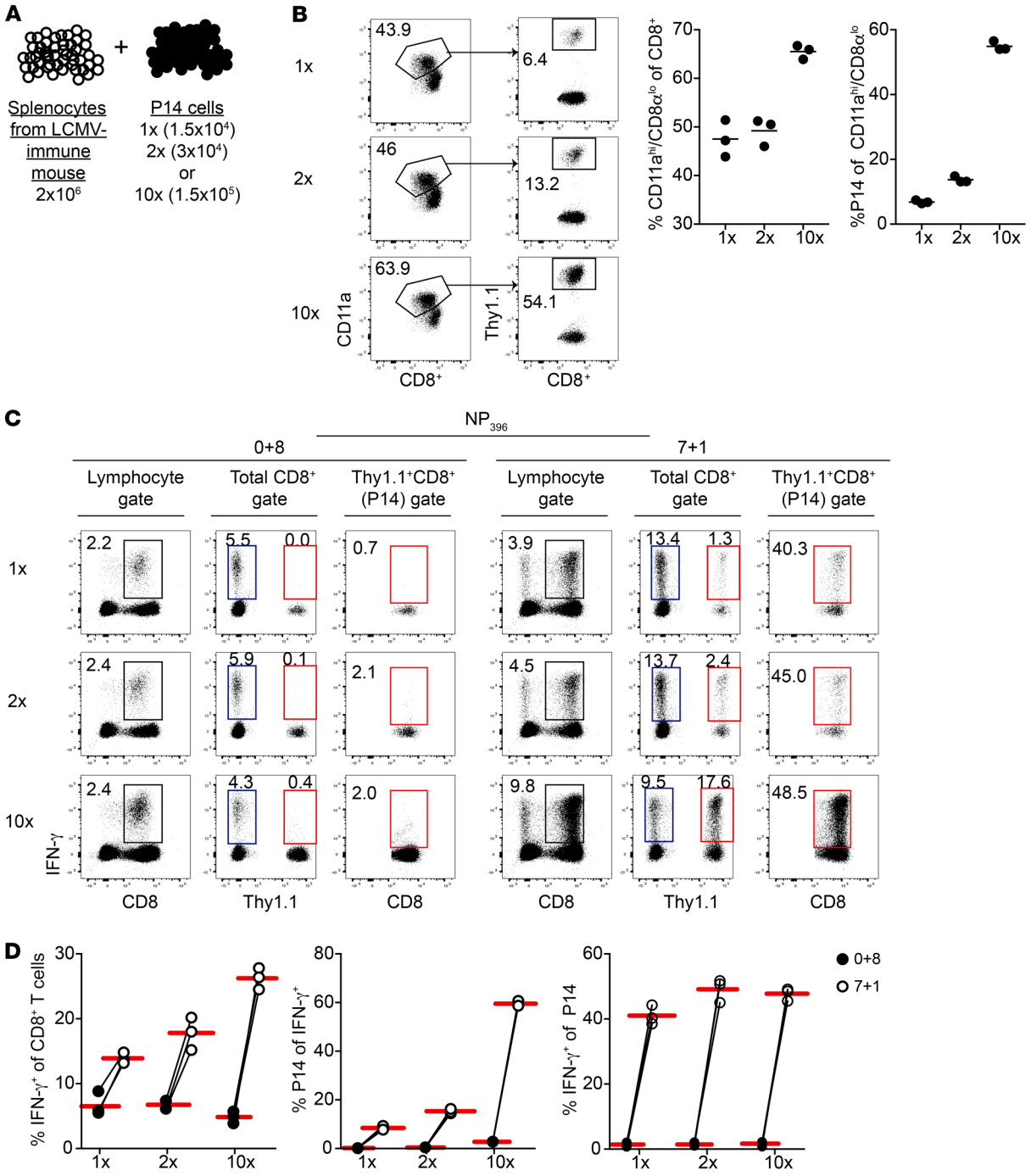

Figure 3. Contribution of bystander responses to IFN-γ–producing cells detected when addition of BFA is delayed is influenced by CD8⁺ T cell pool composition. (**A**) Experimental design. Before 8-hour incubation with NP_{396} peptide, splenocytes from an LCMV-Armstrong–immune mouse were mixed with different numbers of sorted memory P14 cells. (**B**) Left: Representative dot plots of Ag-experienced ($CD11a^{hi}CD8^{lo}$) $CD8^+$ T cells among all $CD8^+$ T cells (left plot) and percentage of P14 cells ($Thy1.1^+$) among Ag-experienced $CD8^+$ T cells (right plot) after mixing. Middle: Summary graph of the percentage of Ag-experienced $CD8^+$ T cells among all $CD8^+$ T cells after mixing. Right: Summary graph of the percentage of memory P14 cells among Ag-experienced $CD8^+$ T cells after mixing. (**C**) Representative dot plots of IFN-γ production following 8-hour incubation with NP_{396} peptide and with BFA present for the entire incubation (0+8) or the final hour (7+1). Plots on the left are gated lymphocytes, plots in the middle are gated $CD8^+$ T cells ($Thy1.1^-$ = endogenous $CD8^+$ T cells, $Thy1.1^+$ = P14 cells), and plots on the right are gated P14 cells. Numbers inside plots indicate the percentage of cells producing IFN-γ out of all gated cells. (**D**) Left: Summary graphs of the percentage of $CD8^+$ T cells producing IFN-γ out of all $CD8^+$ T cells with BFA present for the entire incubation (0+8) or the final hour (7+1). Middle: Summary graphs of the percentage of P14 cells producing IFN-γ out of all IFN-γ^+ $CD8^+$ T cells with BFA present for the entire incubation (0+8) or the final hour (7+1). Right: Summary graphs of the percentage of gated P14 cells producing IFN-γ with BFA present for the entire incubation (0+8) or the final hour (7+1). Representative data from 2 independent experiments. *n* = 3. Dots indicate individual mice. Solid red lines indicate the mean.

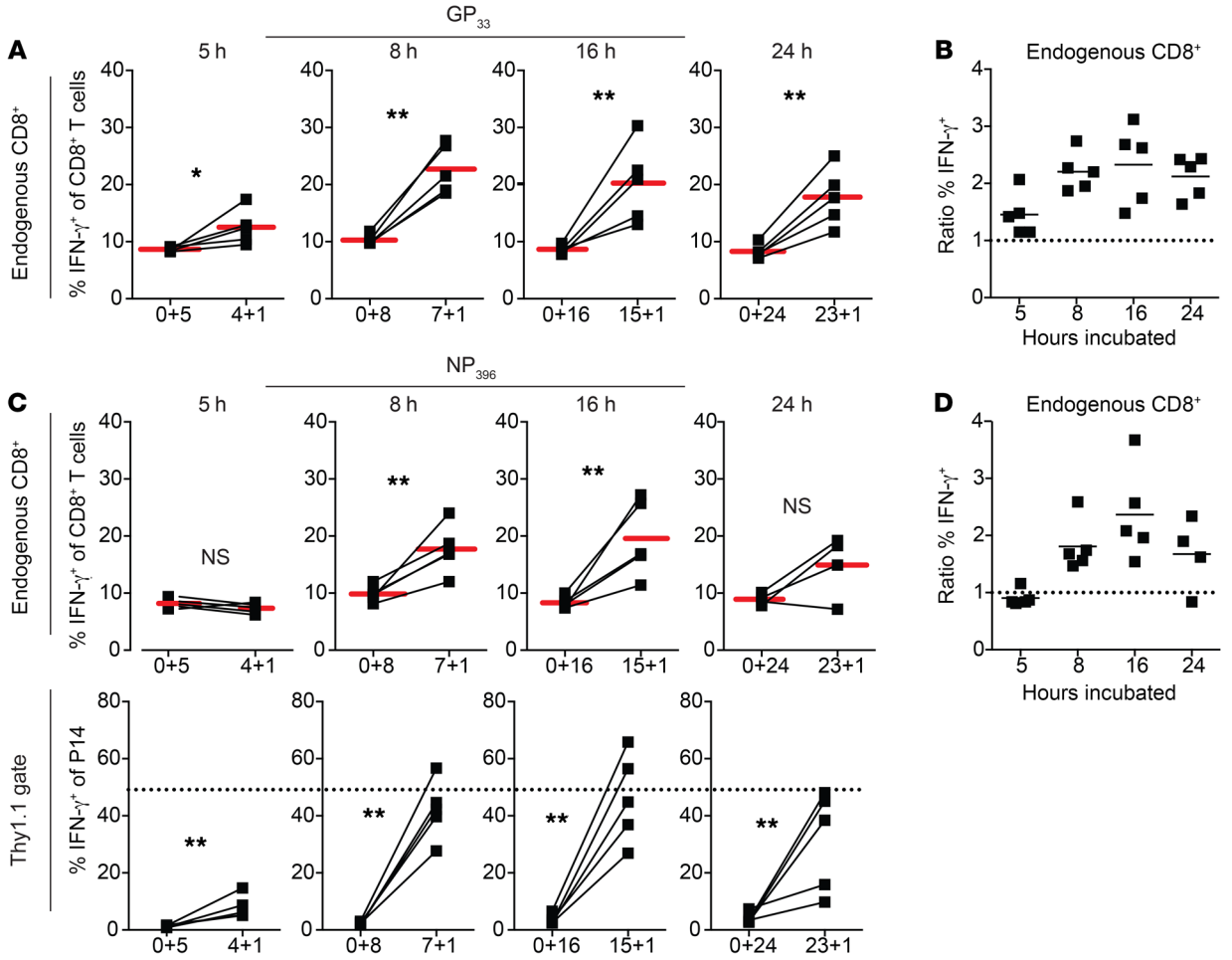

Figure 4. Contribution of bystander responses to IFN-γ–producing cells detected when BFA addition is delayed increases with extended length of stimulation but is seen following incubation times of 5 or more hours. Mice received adoptive transfer of naive P14 cells and were infected with LCMV-Armstrong. ICS was conducted with GP_{33} (**A** and **B**) or NP_{396} (**C** and **D**) peptide approximately 3 weeks after infection. Total incubation times were 5, 8, 16, or 24 hours with BFA present for the whole incubation or the final hour. (**A**) Summary graphs of the percentage of endogenous (Thy1.1$^-$) CD8$^+$ T cells producing IFN-γ out of all endogenous CD8$^+$ T cells with BFA present for the entire incubation or the final hour. (**B**) Ratio of the percentage of endogenous CD8$^+$ T cells producing IFN-γ when BFA was present for the final hour of incubation over the percentage of endogenous CD8$^+$ T cells producing IFN-γ when BFA was present for the entire incubation. (**C**) Top: Summary graphs of the percentage of endogenous (Thy1.1$^-$) CD8$^+$ T cells producing IFN-γ out of all endogenous CD8$^+$ T cells with BFA present for the entire incubation or the final hour. Bottom: Summary graphs of the percentage of P14 cells (Thy1.1$^+$) producing IFN-γ out of all P14 cells with BFA present for the entire incubation or the final hour. (**D**) Ratio of the percentage of endogenous CD8$^+$ T cells producing IFN-γ when BFA was present for the final hour of incubation over the percentage of endogenous CD8$^+$ T cells producing IFN-γ when BFA was present for the entire incubation. Representative data from more than 3 independent experiments. $n = 5$. Dots indicate individual mice. Solid lines indicate the mean. $^*P < 0.05$, $^{**}P < 0.01$ as determined by paired Student's t test.

cells in response to NP_{396} peptide stimulation. While few IFN-γ–producing P14 cells were detected following stimulation with NP_{396} peptide in the presence of BFA for the entire incubation, 25%–30% of memory P14 cells produced IFN-γ in response to NP_{396} peptide when BFA was not present during the whole incubation time (Figure 2D, red boxes). Analyses of T cell responses by ICS in human samples often rely on stimulation for greater than 8 hours, with addition of BFA before the last hour of incubation. To determine whether bystander responses contribute to IFN-γ–producing cells detected for incubation times of greater length and when BFA is added earlier in the culture, we stimulated splenocytes from LCMV-immune mice that contained memory P14 cells with NP_{396} peptide for 8 hours and added BFA after 4 or 7 hours, or for 12 hours and added BFA after 4, 8, or 11 hours. Bystander responses by P14 cells could be detected when BFA was added before the last hour and when cells were stimulated for 8 or more hours, and bystander responses increased with greater length of stimulation in the absence of BFA (Supplemental Figure 2). Thus, delayed addition of BFA in both the mouse and human models of viral and malaria-specific CD8$^+$ T cells can result in bystander activation of Ag-experienced CD8$^+$ T cells leading to inflation in frequencies and numbers of Ag-specific CD8$^+$ T cells detected.

Contribution of bystander IFN-γ activation is dependent on CD8$^+$ T cell pool composition and length of stimulation. Ag-experienced CD8$^+$ T cells can undergo bystander activation and produce cytokines such as IFN-γ, while naive CD8$^+$ T cells cannot (40, 46). Notably, the representation of Ag-experienced cells within the CD8$^+$ T cell pool in human subjects can vary widely based on

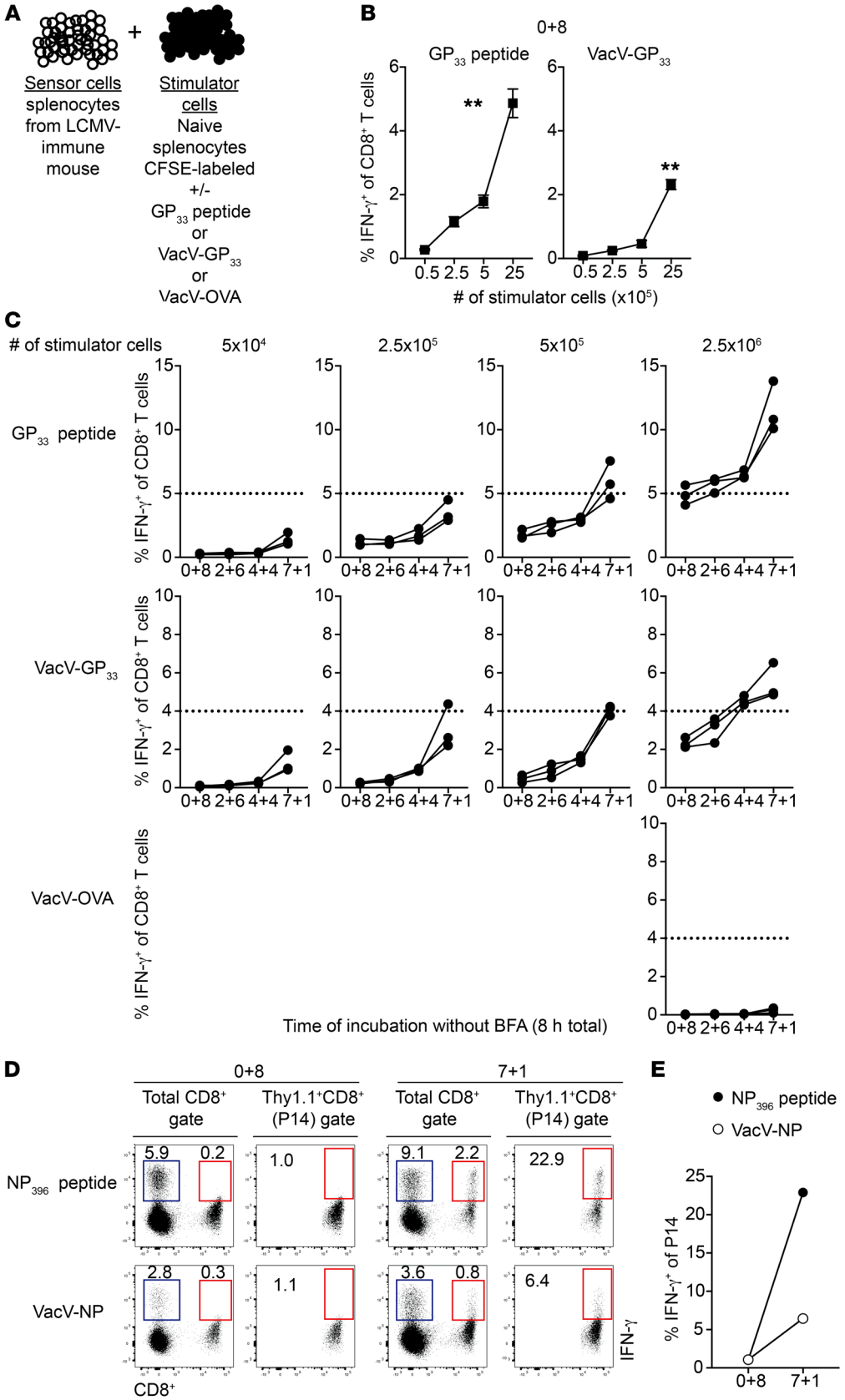

Figure 5. Delayed BFA addition leads to bystander activation of CD8⁺ T cells following stimulation with pathogen-infected splenocytes. (**A**) Experimental design. Splenocytes from a naive mouse (stimulator cells) were CFSE-labeled and either pulsed with GP_{33} peptide or infected with VacV-GP_{33} or VacV-OVA. Stimulator cells were mixed with splenocytes from an LCMV-Armstrong–immune mouse (sensor cells) and incubated for 8 hours with BFA present for 8 (0+8), 6 (2+6), 4 (4+4), or 1 (7+1) hours. (**B**) CD8⁺ T cells producing IFN-γ after 8-hour incubation with indicated numbers of GP_{33} peptide–pulsed (left) or VacV-GP_{33}–infected (right) stimulator cells with BFA present for the entire incubation. (**C**) Top: CD8⁺ T cells producing IFN-γ after incubation with indicated numbers of GP_{33} peptide–pulsed stimulator cells and with BFA for the indicated times. Middle: CD8⁺ T cells producing IFN-γ after incubation with indicated numbers of VacV-GP_{33}–infected stimulator cells and with BFA for the indicated times. Bottom: CD8⁺ T cells producing IFN-γ after incubation with the indicated number of VacV-OVA–infected stimulator cells and with BFA for the indicated times. (**D**) NP_{396} peptide–pulsed or VacV-NP–infected stimulator cells were mixed with sensor cells from an LCMV-Armstrong–immune mouse containing P14 cells. Representative dot plots of IFN-γ production by gated CD8⁺ T cells (left plots: Thy1.1⁻ = endogenous CD8⁺ T cells, Thy1.1⁺ = P14 cells) or P14 cells (right plots). Numbers inside plots indicate the percentage of cells producing IFN-γ out of all gated cells. (**E**) Summary graph of the percentage of P14 cells producing IFN-γ after stimulation with NP_{396}-pulsed (black circles) or VacV-NP–infected stimulator cells (white circles) with BFA present for the entire incubation (0+8) or the final hour (7+1). Representative data from 3 independent experiments. $n = 3$. Dots indicate individual mice. $^{**}P < 0.01$ as determined by paired Student's t test.

age and history of previously encountered infections (47, 48). To determine whether the composition of Ag experience in the $CD8^+$ T compartment dictated frequencies of IFN-γ–producing $CD8^+$ T cells, we manipulated the number of Ag-experienced cells among splenocytes by mixing splenocytes from LCMV-immune mice with graded numbers of sorted memory P14 "sensor" cells to achieve different ratios of naive ($CD11a^{lo}CD8^{hi}$) to memory ($CD11a^{hi}CD8^{lo}$) $CD8^+$ T cells (refs. 49, 50, and Figure 3, A and B). Again, few IFN-γ–producing P14 cells were detected following stimulation with NP_{396} peptide when BFA was present for the entire incubation, and a similar percentage of $CD8^+$ T cells producing IFN-γ in response to NP_{396}-peptide stimulation was observed regardless of numbers of P14 cells present (Figure 3, C and D, 0+8 group). However, when BFA was not present for the entire incubation, the percentage of IFN-γ–producing $CD8^+$ T cells in response to NP_{396} peptide stimulation increased with increasing numbers of sensor P14 cells, and this was due to increased representation of P14 cells rather than elevation in the frequency of activated bystander P14 cells (Figure 3, C and D, 7+1 group). Thus, the contribution of bystander-activated cells to the IFN-γ–producing $CD8^+$ T cell population was dependent on the representation of Ag-experienced cells within the $CD8^+$ T cell compartment. These data suggested that the increase in the frequency of vaccine-targeted memory $CD8^+$ T cells might be more pronounced in older subjects and/or subjects with substantial history of pathogen exposures that possess more previously activated $CD8^+$ T cells.

The duration of Ag stimulation ex vivo for experiments involving human subjects varies, but in most instances stimulation times are between 5 and 24 hours (4, 6, 9–39). To determine whether the duration of stimulation contributes to the degree of bystander IFN-γ detected when BFA is not present for the entire incubation, splenocytes from an LCMV-immune mouse were incubated with GP_{33} or NP_{396} peptides for 5, 8, 16, or 24 hours with BFA present for the entire incubation or for the final hour of incubation. Regardless of length of incubation, a greater percentage of IFN-γ–producing $CD8^+$ T cells was detected following stimulation with GP_{33} (Figure 4, A and B) or NP_{396} (Figure 4, C and D) peptides when BFA was added for only the last hour of incubation. However, increased detection of IFN-γ–producing $CD8^+$ T cells was most pronounced when samples were incubated for greater than 5 hours. Similarly, bystander-activated P14 cells were detected in response to NP_{396} peptide stimulation when BFA addition was delayed for any length of incubation tested, but percentages of bystander-activated P14 cells detected were greater when samples were incubated for greater than 5 hours (Figure 4C). These data suggested that bystander activation occurred and contributed to the frequency of IFN-γ–producing $CD8^+$ T cells detected when BFA was not present for the entire incubation across the spectrum of incubation times used to conduct ICS. However, the contribution of bystander-activated cells to IFN-γ–producing cells detected is likely to increase with greater lengths of incubation.

Delayed addition of BFA leads to bystander activation of Ag-experienced $CD8^+$ T cells following stimulation with whole pathogen. Application of peptide-stimulated ICS assays across individual human subjects assessing responses to complex pathogens with many antigens is difficult because of differences in HLA haplotype; thus, stimulation of human samples is often achieved by exposing samples to whole pathogens (Figure 1), or through the use of libraries of long overlapping peptides, methods that may require a period of BFA-free culture to allow for optimal Ag processing and presentation or cross-presentation. To determine whether bystander-activated cells contributed to the frequency of IFN-γ–producing cells detected after stimulation with whole pathogens, splenocytes from an LCMV-immune mouse ("sensor" cells) were incubated with CFSE-labeled splenocytes that were either pulsed with GP_{33} peptide or infected with Vaccinia virus (VacV) expressing cognate Ag (VacV-GP_{33}) or an irrelevant Ag (VacV-OVA) (Figure 5A). When BFA was present throughout the incubation period, IFN-γ production from the LCMV-immune sensor cells was observed in response to spleen cells pulsed with GP_{33} peptide or infected with VacV-GP_{33}, and the percentage of IFN-γ–producing $CD8^+$ T cells detected increased with increasing numbers of stimulator cells added to the culture (Figure 5B). IFN-γ production was not observed in response to splenocytes infected with VacV-OVA (Figure 5C, bottom).

Interestingly, an increased percentage of IFN-γ–producing sensor cells were detected following incubation with greater numbers of GP_{33}-pulsed or VacV-GP_{33}–infected stimulator cells and when addition of BFA was delayed for longer periods (Figure 5C, top and middle). These data suggested that length of incubation with BFA impacted detection of IFN-γ–producing $CD8^+$ T cells following stimulation with pathogen-infected splenocytes. However, because we could not determine whether our stimulation conditions resulted in IFN-γ production by bona fide Ag-specific or any Ag-experienced $CD8^+$ T cells, we were unable to conclude whether delayed addition of BFA resulted in increased detection of true Ag-specific $CD8^+$ T cells, or whether increased percentages of IFN-γ–producing $CD8^+$ T cells detected were due to bystander activation of memory $CD8^+$ T cells. To address this, we incubated sensor cells from LCMV-immune P14 chimera mice with stimulator cells that were either pulsed with NP_{396} peptide or infected with VacV expressing LCMV nucleoprotein (VacV-NP). An increased percentage of IFN-γ–producing cells was detected following stimulation with peptide-pulsed or VacV-NP–infected cells when BFA was not present for the whole incubation time (Figure 5, D and E). Importantly, in the same samples, GP_{33}-specific P14 memory $CD8^+$ T cells produced IFN-γ in response to VacV-NP–infected splenocytes, strongly suggesting Ag-independent bystander activation. Thus, stimulation with whole pathogens, while not as potently as peptide stimulation, also resulted in bystander $CD8^+$ T cell activation, and the potential for inaccurate accounting of pathogen/vaccine-specific $CD8^+$ T cell responses.

Blocking inflammatory cytokines limits bystander activation of $CD8^+$ T cells. Bystander IFN-γ production by effector or memory $CD8^+$ T cells can be stimulated by hundreds of inflammatory cytokine combinations (42). As an example, a large percentage of endogenous and P14 memory $CD8^+$ T cells derived from LCMV-immune P14 chimera mice produced IFN-γ in response to IL-12 and IL-18, IL-12 and TNF-α, or IL-12 and IL-15 stimulation alone, but only when BFA was not present during the entire incubation (Figure 6A and Supplemental Figure 3, A and B). Similarly, addition of IL-12 and IL-18 significantly increased the frequency of IFN-γ–producing $CD8^+$ T cells even in the presence of peptide (GP_{33} in Figure 6B and NP_{396} in Figure 6C) stimulation, but only if BFA addition was delayed. Notably, addition of IL-12

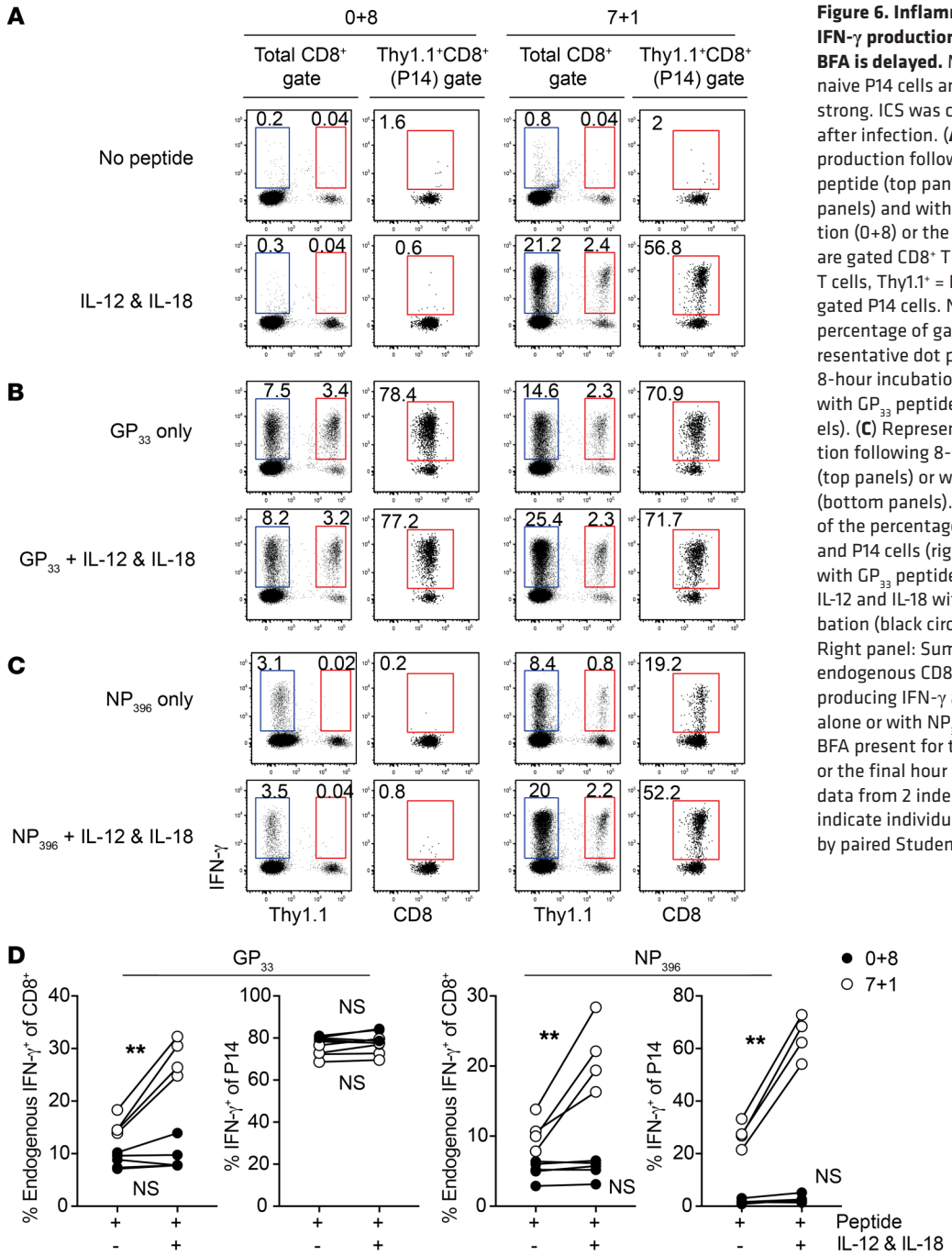

Figure 6. Inflammatory cytokines trigger bystander IFN-γ production by CD8⁺ T cells when addition of BFA is delayed. Mice received adoptive transfer of naive P14 cells and were infected with LCMV-Armstrong. ICS was conducted approximately 3 weeks after infection. (**A**) Representative dot plots of IFN-γ production following 8-hour incubation without peptide (top panels) or with IL-12 and IL-18 (bottom panels) and with BFA present for the entire incubation (0+8) or the final hour (7+1). Plots on the left are gated CD8⁺ T cells (Thy1.1⁻ = endogenous CD8⁺ T cells, Thy1.1⁺ = P14 cells), and plots on the right are gated P14 cells. Numbers inside plots indicate the percentage of gated cells producing IFN-γ. (**B**) Representative dot plots of IFN-γ production following 8-hour incubation with GP_{33} peptide (top panels) or with GP_{33} peptide and IL-12 and IL-18 (bottom panels). (**C**) Representative dot plots of IFN-γ production following 8-hour incubation with NP_{396} peptide (top panels) or with NP_{396} peptide and IL-12 and IL-18 (bottom panels). (**D**) Left panel: Summary graphs of the percentage of endogenous CD8⁺ T cells (left) and P14 cells (right) producing IFN-γ after incubation with GP_{33} peptide alone or with GP_{33} peptide and IL-12 and IL-18 with BFA present for the entire incubation (black circles) or the final hour (white circles). Right panel: Summary graphs of the percentage of endogenous CD8⁺ T cells (left) and P14 cells (right) producing IFN-γ after incubation with NP_{396} peptide alone or with NP_{396} peptide and IL-12 and IL-18 with BFA present for the entire incubation (black circles) or the final hour (white circles). Representative data from 2 independent experiments. $n = 4$. Dots indicate individual mice. $^{**}P < 0.01$ as determined by paired Student's t test.

and IL-18 (one of the most potent cytokine combinations that lead to bystander activation) (42) did not increase the number of peptide-stimulated IFN-γ–producing cells (GP_{33} or NP_{396} in Figure 6D) if BFA was present all the time (0+8 group). Furthermore, as described previously, human PBMCs incubated with IL-12 and IL-18 also produced IFN-γ (51–53), but only when BFA was not present during the entire incubation (Supplemental Figure 3, C and D). This suggested that human samples also may be susceptible to inflammation-driven bystander responses, similar to those observed in mice during ICS when BFA is not present for the entire incubation. Thus, accurate detection of Ag-specific human CD8⁺ T cells by ICS may be influenced by timing of BFA addition.

These data also suggest that bystander responses elicited in response to Ag stimulation when BFA is not present in culture for the entire incubation require intact Golgi function. Two possible explanations for the absence of bystander responses in the presence of BFA for the entire culture, then, are (a) that BFA prevents cytokine secretion that elicits bystander responses, or (b) that BFA prevents transport of cytokine receptors to the cell surface, blocking the ability of cells to respond to inflammatory cues. It is also possible that both mechanisms contribute to bystander responses elicited when addition of BFA is delayed. Data presented in Figure 2 and Supplemental Figure 3 suggest that cytokines secreted in response to cognate Ag can drive

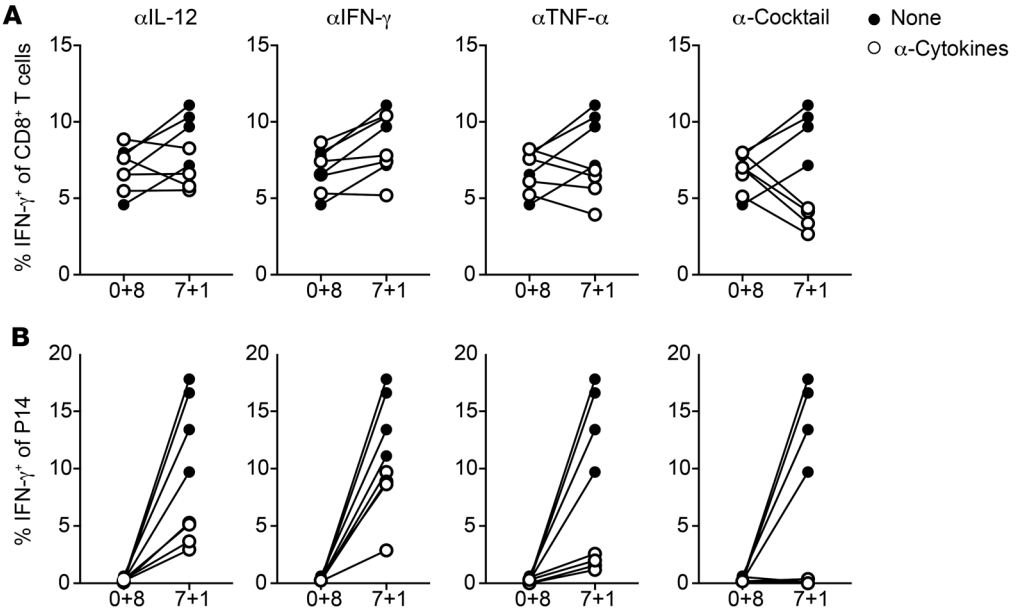

Figure 7. Blocking inflammatory cytokines reduces detection of bystander-activated cells when addition of BFA is delayed. Mice received adoptive transfer of naive P14 cells and were infected with LCMV-Armstrong. ICS was conducted approximately 3 weeks after infection. (**A**) Summary graphs of the percentage of endogenous CD8$^+$ T cells producing IFN-γ after incubation with NP_{396} peptide (black circles) or with NP_{396} peptide and 50 μg anti–IL-12, anti–IFN-γ, anti–TNF-α, or a mix of all anti-cytokines (white circles) with BFA present for the entire incubation (0+8) or the final hour (7+1). (**B**) Summary graphs of the percentage of P14 cells producing IFN-γ after incubation with NP_{396} peptide (black circles) or with NP_{396} peptide and 50 μg anti–IL-12, anti–IFN-γ, anti–TNF-α, or a mix of all anti-cytokines (white circles) with BFA present for the entire incubation (0+8) or the final hour (7+1). Representative data from 2 independent experiments. *n* = 4.

bystander responses when addition of BFA is delayed, as adding noncognate Ag alone is able to induce bystander responses [7+1, Thy1.1$^+$CD8$^+$ (P14) gates]. Additionally, when we analyzed expression of cytokine receptor components, we found that transcript levels of *Il12rb2*, a signaling component of the IL-12 receptor complex that activates STAT4 signaling and whose expression is regulated by inflammatory cytokines (54), and *Tnfrsf1b*, which binds TNF-α and activates NF-κB and MAPK pathways (55), were increased in sorted P14 cells that were activated in a bystander manner in ICS cultures stimulated with NP_{396} peptide where addition of BFA was delayed (Supplemental Figure 4, A and B). Transcript levels of *Ifngr1* and *Ifngr2*, which bind IFN-γ and activate STAT1 pathways (56), were not impacted by delayed addition of BFA in P14 cells (Supplemental Figure 4B), suggesting that the absence of BFA does not sensitize cells capable of undergoing bystander responses to IFN-γ–mediated signaling. However, since IFN-γ receptors are expressed on the surface of nearly all cells, IFN-γ may be acting on other cells in ICS cultures that play a role in driving bystander responses. Thus, delayed addition of BFA during ICS is likely to elicit bystander responses through the combinatorial effects of allowing for secretion of inflammatory cytokines that drive bystander responses into culture media, and allowing for export of inflammatory cytokine receptors to the surface of Ag-experienced cells, which enhances sensitivity to inflammatory cytokines.

A further suggestion from the data presented in Figure 6 is that cytokine blockade during stimulation could enhance the fidelity of detection of bona fide Ag-specific CD8$^+$ T cells by the ICS assay. To test this, splenocytes from LCMV chimera P14 mice were incubated with NP_{396} peptide for 8 hours in the presence of BFA for the entire incubation or for the final hour, with or without anti–IL-12, –IFN-γ, and/or –TNF-α blocking Abs. While incubation of splenocytes in the absence of BFA led to bystander IFN-γ production and increased percentages of IFN-γ–producing CD8$^+$ T cells, addition of a cocktail of cytokine-blocking Abs was maximally effective at limiting bystander responses, and addition of blocking Abs against individual cytokines, to varying degrees, reduced the percentages of endogenous (Figure 7A) or P14 cells (Figure 7B) producing IFN-γ in a bystander manner, thus improving the overall accuracy in detecting Ag-specific memory CD8$^+$ T cells. In summary, these data suggest that blocking inflammatory cytokines during stimulation can reduce the contribution of bystander-activated cells to IFN-γ–producing Ag-specific CD8$^+$ T cells detected by ICS, and may provide for a more accurate estimation of Ag-specific CD8$^+$ T cells using different ICS protocols.

Bystander-activated human CD8$^+$ T cells contribute to IFN-γ–producing cells detected following stimulation with whole pathogens. The data in Figure 5 from the mouse model showed that stimulation with whole pathogens could lead to bystander activation of CD8$^+$ T cells, and the data in Figure 1 from humans showed that there was a higher percentage of IFN-γ–producing cells detected in PfSPZ-vaccinated human subjects following ICS of longer duration and when BFA was added later in the stimulation. To determine whether bystander activation of CD8$^+$ T cells contributed to the pool of IFN-γ–producing CD8$^+$ T cells detected in human subjects, PBMCs from PfSPZ-vaccinated subjects were labeled with CFSE and individually combined at a ratio of 9:1 with PBMCs obtained from the same subjects before vaccination (Fig-

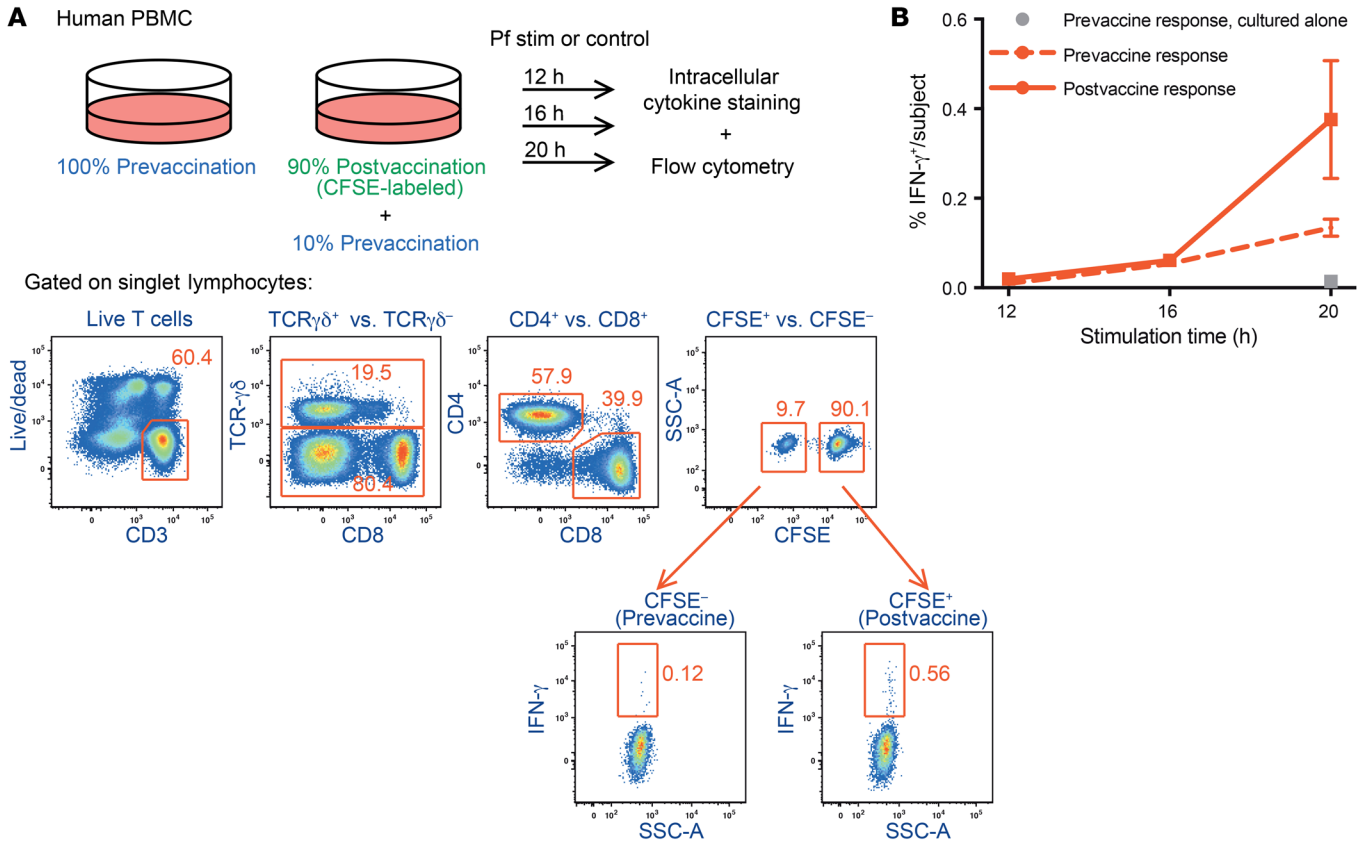

Figure 8. Delayed addition of BFA leads to bystander activation of human CD8⁺ T cells following stimulation with PfSPZs. PBMCs from PfSPZ-vaccinated subjects were CFSE-labeled and mixed with nonlabeled PBMCs from the same subjects (to allow for detection of bystander responses) that were collected before vaccination. Samples were then stimulated with PfSPZs for 12, 16, or 20 hours, and BFA was added for the last 4 hours of the incubation. PBMCs from subjects before vaccination were also stimulated in the absence of postvaccination samples as a control. (**A**) Experimental design (top) and representative dot plot of the mix of preimmunization ($CFSE^-$) and postimmunization ($CFSE^+$) PBMCs (bottom) following stimulation for 20 hours with PfSPZs. (**B**) Percentage of IFN-γ–producing cells detected among prevaccine samples cultured alone (control), among prevaccine cells (bystander responses) cultured with postvaccine cells, and among postvaccine cells cultured with prevaccine cells following stimulation. $n = 3$. Data are mean ± SEM.

ure 8A). This design allows for detection of bystander responses, as any IFN-γ–producing cells in the prevaccine population of cells could only be due to noncognate Ag-driven responses. Cells were then incubated with PfSPZs for 12, 16, or 20 hours in the presence of BFA for the last 4 hours. While IFN-γ–producing $CD8^+$ T cells were low to undetectable when prevaccine PBMCs were cultured in the absence of postvaccine PBMCs, a significant percentage of prevaccine PBMCs produced IFN-γ when cultured with postvaccination PBMCs (Figure 8B). These data showed that, under conditions of stimulation used most commonly for detection of $CD8^+$ T cells by the ICS assay from subjects that receive whole sporozoite vaccine (57, 58), bystander activation of human $CD8^+$ T cells can confound the enumeration of bona fide pathogen/vaccine-induced memory $CD8^+$ T cells.

Notably, design of whole-pathogen stimulation assays for mice shown in Figure 5, in which infection of stimulator splenocytes occurred prior to mixing with sensor cells of interest, was different from design of the human assays shown in Figure 8, in which whole pathogen was added directly to cells of interest at the initiation of culture. To determine whether bystander responses in mice following whole pathogen stimulation also contributed to IFN-γ–producing cells detected when whole pathogens were added directly to samples being analyzed, we designed experiments shown in Supplemental Figure 5, A and D. With 2 different models, activation of P14 cells following stimulation with the bacterium *Listeria monocytogenes* (LM-OVA/B8R) (Supplemental Figure 5B) and activation of OT-I cells following stimulation with Vaccinia virus (VacV-GP_{33}) (Supplemental Figure 5E), bystander responses contributed to IFN-γ–producing cells detected. Furthermore, addition of cytokine-blocking Abs reduced the contribution of bystander P14 responses detected (Supplemental Figure 5C).

Additionally, to determine whether bystander responses in mice influenced evaluation of $CD8^+$ T cell responses elicited following experimental malaria vaccination, we performed ICS using GAP50 peptide, which is a *Plasmodium berghei*–derived epitope for which naive C57BL/6 mice possess a large Ag-specific naive $CD8^+$ T cell repertoire (59), with splenocytes from mice that were inoculated with radiation-attenuated *P. berghei* sporozoites and that contained memory P14 cells generated in response to prior infection with LCMV (Supplemental Figure 6A). The size of the $CD8^+$ T cell response detected, and contribution of bystander-activated cells to IFN-γ–producing cells detected, increased with increasing length of incubation in the absence of BFA (Supplemental Figure 6, B and C). Thus, modified mouse models recapitulate the

findings observed with human cells, suggesting that bystander responses can contribute to IFN-γ–producing cells detected when addition of BFA is delayed.

Lastly, to determine whether addition of cytokine-blocking Abs may be useful in limiting contribution of bystander responses to human Ag-specific CD8$^+$ T cells detected by ICS when addition of BFA is delayed, we performed ICS with human PBMCs obtained at the University of Iowa DeGowin Blood Center using peptide pools containing CMV- and EBV-derived epitopes. Percentages of IFN-γ–producing cells detected were elevated when addition of BFA was delayed (Supplemental Figure 7, A and B, black dots compared with white dots), suggesting that bystander responses were contributing to Ag-specific cells detected when BFA addition was delayed. However, percentages of IFN-γ–producing cells detected were not significantly different between samples incubated in the presence of BFA from the beginning of stimulation and samples for which addition of BFA was delayed but for which cytokine-blocking Abs were added to ICS cultures (Supplemental Figure 7, A and B, black dots compared with red dots). These data suggest that addition of cytokine-blocking Abs during ICS may be useful for accurate assessment of numbers of true Ag-specific human CD8$^+$ T cells using ICS.

Discussion

The frequency and phenotype of Ag-specific memory CD8$^+$ T cells present prior to infection impact the host's ability to fight pathogenic microorganisms. Therefore, accurately identifying Ag-specific memory CD8$^+$ T cells generated in response to vaccination will facilitate vaccine development, for example, through accurate assessment of the immune correlates of protection. Additionally, assays that seek to further characterize the CD8$^+$ T cell response, for example, by determining expression of phenotypic markers on IFN-γ–producing cells by multiparameter flow cytometry or by sorting activated cells and performing single-cell RNA sequencing may be misled by incorrect identification of bona fide Ag-specific CD8$^+$ T cells.

Here we have shown that, when ICS is used to detect CD8$^+$ T cell responses, bystander activation of Ag-experienced CD8$^+$ T cells can occur when BFA is not present for the entire period of stimulation. Bystander activation was seen in both mouse and human models of viral and malaria infection as well as bacterial infection in mice, and was influenced by the length of stimulation with peptides and whole pathogens. Notably, the contribution of bystander-activated cells to the IFN-γ–producing CD8$^+$ T cell population depended on the frequency of Ag-experienced CD8$^+$ T cells in the sample. Thus, the overrepresentation of Ag-specific CD8$^+$ T cells when ICS is performed without BFA for the entire incubation period will vary depending on the individual examined. However, delaying addition of BFA in human samples may be unavoidable when the Ag sources are whole pathogens/proteins that require undisrupted cell machinery for efficient Ag processing and presentation or cross-presentation. In these cases, addition of cytokine-blocking Abs to ICS cultures may aid in minimizing bystander responses and result in greater accuracy for detection of true Ag-specific responses.

This study does have limitations. A number of additional parameters that may vary in ICS protocols have the potential to impact readout of IFN-γ–producing cells detected, such as number of T cells in culture, representation of Ag-presenting cells, media used, and instrumentation. This is not an exhaustive list, and we were unable to test the impact of every parameter on ICS readout. Furthermore, while we did examine a number of different incubation lengths and timings of BFA addition, we did not exhaustively test how length of incubation and timing of BFA addition impact bystander activation during ICS culture. We were able to detect bystander responses across a range of incubation times from 5 to 24 hours with addition of BFA as early as 4 hours after initiation of ICS (Figure 4 and Supplemental Figure 2). However, bystander responses became magnified with incubations of greater length and with addition of BFA at later times after onset of culture. Thus, choosing incubation times of shorter duration with addition of BFA at earlier times, when possible depending on the nature of the stimulation, may be an additional method to improve accuracy of detection of true Ag-specific responses by ICS.

If ICS assay is providing inaccurate estimates of memory CD8$^+$ T cells present within the host, are other techniques available that might provide a more accurate estimate? An alternative assay for measuring Ag-specific T cell responses, the ELISpot assay, is similarly compromised by bystander activation. While ELISpot is generally considered to be more sensitive than ICS, and thus better suited for detection of rare Ag-specific cells (60), like ICS, it relies on detection of IFN-γ–producing CD8$^+$ T cells following incubation with cognate peptide. Additionally, ELISpot assays commonly have incubation periods lasting for 18 to 48 hours, and such long incubation periods are likely to further exacerbate the bystander activation phenomenon.

Peptide-MHC tetramer staining is also used to measure Ag-specific T cell responses. Unlike ICS conducted following stimulation with antigenic peptide pools or whole pathogens, tetramer staining must be tailored to individual subjects because of differences in MHC haplotypes among individuals (61). Therefore, especially for complex pathogens with thousands of proteins, such as malaria, it can be more logistically challenging than ICS, which can be performed similarly in disparate hosts. Furthermore, tetramer staining marks Ag-specific cells with limited information about cell functionality. Following ICS with GP_{33} peptide, only about 80% of P14 cells that are known to recognize the GP_{33} epitope of LCMV responded with IFN-γ production (Figures 2 and 6), suggesting that some memory cells within the host are not capable of performing effector functions. At least some of these cells are likely to be T death-intermediate memory (T_{DIM}) cells, which are generated during the process of homeostatic memory cell turnover, and are incapable of IFN-γ production or release of cytotoxic granules (62). Because host protection is ultimately dependent on the number of cells present that are capable of responding to invading microbes with effector functions, ICS may provide a more accurate measure of protection than tetramer staining, as the former detects only cells capable of executing effector functions, while the latter detects cells that may be nonfunctional.

How can ICS be tailored to provide a more accurate assessment of Ag-specific CD8$^+$ T cell responses? Reductions in bystander activation can be achieved by selecting the shortest possible length of incubation and by adding BFA at the beginning of stimulation. However, when inclusion of BFA at the onset of ICS is not

feasible because of stimulation with whole pathogen or proteins that require processing, additional steps can be performed to reduce bystander activation and provide a more accurate enumeration of bona fide Ag-specific $CD8^+$ T cells. The severity of bystander activation can be mitigated by allowing pathogen processing and presentation to proceed first in a pure culture of Ag-presenting cells prior to the concurrent addition of syngeneic T cells and BFA. If such a strategy is not feasible, blocking antibodies against cytokines detected in the supernatant could be added during incubation to reduce bystander activation and increase accuracy.

Taking these steps to ensure accurate detection of Ag-specific effector or memory $CD8^+$ T cells will likely aid in evaluation and design of vaccines for infections of global importance and for cancer immunotherapy.

Methods

Human subjects, PfSPZ vaccination, and collection of PBMCs. Human samples from malaria-vaccinated or naive subjects were obtained from the VRC 314 study, as previously described (63). Briefly, healthy US adult volunteers were vaccinated i.v. with the PfSPZ vaccine (64). EDTA-anticoagulated whole blood was collected before vaccination and after the final vaccination. PBMCs were isolated by density gradient centrifugation and cryopreserved in liquid nitrogen vapor phase.

Mice, infections, and generation of memory $CD8^+$ T cells. Inbred female C57BL/6 mice were purchased from the National Cancer Institute (Frederick, Maryland, USA) and bred at the University of Iowa, and TCR-Tg P14 and OT-I mice were bred at the University of Iowa. All mice were used at 6–10 weeks of age and housed at the University of Iowa at appropriate biosafety levels.

All LCMV-Armstrong infections were performed i.p. with 2×10^5 PFU per mouse. All *Listeria monocytogenes* (LM) infections were performed i.v. (retro-orbital injection) with 1×10^7 CFU per mouse of attenuated (Att) LM expressing the OVA_{257} peptide and the full-length B8R protein from Vaccinia virus (VacV) (LM-OVA/B8R). For infections with radiation-attenuated *P. berghei* sporozoites (Pb-RAS), *P. berghei* ANKA clone 234 sporozoites were isolated from the salivary glands of *Anopheles stephensi* mosquitos purchased from the insectary of New York University. Sporozoites were attenuated by radiation with 200 Gy by cesium irradiation prior to i.v. (retro-orbital) injection of 2×10^4 sporozoites per mouse. In vitro infections were performed using VacV expressing the OVA_{257} peptide (VacV-OVA), the GP_{33} peptide (VacV-GP_{33}), or the full-length nuclear protein (NP) from LCMV (VacV-NP; obtained from Steven Varga, Department of Microbiology and Immunology, University of Iowa, Iowa City, Iowa, USA), or LM-OVA/B8R expressing the full-length OVA peptide and B8R peptide derived from VacV (obtained from J.D. Sauer, Department of Medical Microbiology and Immunology, University of Wisconsin, Madison, Wisconsin, USA).

Primary memory P14 cells were generated by adoptive transfer of 5×10^3 P14 cells obtained from peripheral blood of naive P14 mice (Thy1.1/1.1 or Thy1.1/1.2) into naive C57BL/6 recipients (Thy1.2/1.2) followed by infection with LCMV. Primary memory OT-I cells were generated by adoptive transfer of 5×10^3 OT-I cells obtained from peripheral blood of naive OT-I mice (Thy1.1/1.1 or Thy1.1/1.2) into naive C57BL/6 recipients (Thy1.2/1.2) followed by infection with LM-OVA/B8R.

ICS and flow cytometry for human and mouse samples. For Figure 1, 1.5×10^6 PBMCs from PfSPZ-immunized or nonimmunized (naive) subjects were incubated with 1.5×10^5 PfSPZs for the durations indicated. BFA (GolgiPlug, BD Biosciences catalog 555029) was added to the culture medium at the times indicated at 10 μg/mL.

For Figure 8, postvaccination PBMCs were CFSE-labeled and mixed at a 9:1 ratio with preimmunization PBMCs, and a total of 1.5×10^6 PBMCs were incubated with 1.5×10^5 PfSPZs for the times indicated, and with addition of BFA for the last 4 hours of incubation.

After stimulation, cells were stained as previously described (65). Briefly, cells were stained for viability with Aqua Live-Dead dye (Invitrogen), surface-stained with CCR7 (clone Ax680, NIH Vaccine Research Center), CD3 (clone SP34.2, BD Biosciences), TCRγδ (clone B1, BD Biosciences), CD4 (clone OKT4, BioLegend), CD8 (clone RPA-T8, BioLegend), and CD45RA (clone MEM-56, Invitrogen), and stained intracellularly for IFN-γ (clone 4S.B3, BioLegend), IL-2 (clone MQ1-17H12, BioLegend), and TNF-α (clone Mab11, BioLegend). Flow cytometry data were acquired using a modified LSR-II cytometer (BD Biosciences) and analyzed using FlowJo version 9.9.6 software (Tree Star Inc.).

For human PBMCs examined in Supplemental Figures 3 and 7, LRS cones from a Trima Accel automated blood collection system (Terumo BCT) were used to remove PBMCs, and the LRS cones were provided to investigators at the University of Iowa by the DeGowin Blood Center. PBMCs from cones were flushed by washing with complete RPMI followed by red blood cell lysis with ACK lysis buffer. PBMCs were then washed 3 times with complete RPMI and filtered through a 70-μm cell strainer before being resuspended in freezing media (90% FBS and 10% DMSO) and stored at –80°C. Cells were revived from frozen stocks by being thawed in a water bath followed by suspension in warmed complete media. Cells were then washed 3 times in warmed media and strained through a 70-μm cell strainer before 2×10^6 cells were plated and incubated. For Supplemental Figure 3, cells were incubated with or without 100 ng/mL human rIL-12 (BD Biosciences) and IL-18 (Medical and Biological Laboratories) for a total of 8 hours with BFA present for the entire incubation (0+8) or for the final hour (7+1), or for a total of 20 hours with BFA present for the entire incubation (0+20) or for the final 4 hours (16+4). For Supplemental Figure 7, cells were incubated with or without 200-nM concentrations of peptide pools consisting of CMV pp50 peptide (VTEHDTLLY, presented by HLA-A*0101 allele), CMV pp65 peptide (NLVPMVATV, presented by HLA-A*0201 allele), and EBV BMLF-1 peptide (GLCTLVAMD, presented by HLA-A*0201 allele) (all purchased from IBA Lifesciences), and with or without 0.6 μg/mL anti–IFN-γ, 0.6 μg/mL anti–TNF-α, 9 μg/mL anti–IL-12, and 9 μg/mL anti–IL-18 (all from R&D Systems), for a total of 20 hours with BFA present for the entire incubation (0+20) or for the final 4 hours (16+4). Cells were stained for surface expression of CD45RA (clone HI100, BioLegend), CD4 (clone A161A1, BioLegend), CD8 (clone HIT8a, BioLegend), and CD3 (clone HIT3a, BioLegend) and intracellular expression of IFN-γ (clone 4S.B3, BioLegend).

For mouse samples, spleens were collected and tissue was processed into single-cell suspension. Unless otherwise stated (Supplemental Figure 1), 2×10^6 splenocytes were incubated with 200-nM concentrations of GP_{33}, NP_{396}, or $GAP50_{40}$ peptide. Unless otherwise stated (Figures 4 and 5 and Supplemental Figures 2, 5, and 6), samples were incubated for a total of 8 hours with BFA present for the entire incubation (0+8) or for the final hour of incubation (7+1). In Figure 4,

cells were incubated for a total of 5, 8, 16, or 24 hours with BFA present for the entire incubation or for the final hour of incubation. In Figure 5, cells were incubated for a total of 8 hours with BFA present for the entire incubation (0+8), for the final 6 hours of incubation (2+6), for the final 4 hours of incubation (4+4), or for the final hour of incubation (7+1). In Supplemental Figure 2, cells were incubated for a total of 8 hours with BFA present for the entire incubation (0+8), for the final 4 hours of incubation (4+4), or for the final hour of incubation (7+1); or for a total of 12 hours with BFA present for the entire incubation (0+12), for the final 8 hours of incubation (4+8), for the final 4 hours of incubation (8+4), or for the final hour of incubation (11+1). In Supplemental Figure 5, cells were incubated for a total of 12, 16, or 20 hours with BFA present for the final 4 hours of incubation. In Supplemental Figure 6, cells were incubated for a total of 12 hours with BFA present for the entire incubation (0+12), for the final 8 hours of incubation (4+8), for the final 4 hours of incubation (8+4), or for the final hour of incubation (11+1).

In Figure 3, P14 cells that were positively selected were added to splenocytes from an LCMV-immune mouse before incubation. For positive selection, cells were stained with PE–anti-Thy1.1 Abs (clone His51, eBioscience) and purified with anti-PE magnetic bead sorting using standard AutoMacs protocols.

In Figure 6, splenocytes were incubated with or without 10 ng/mL rIL-12 and IL-18 (R&D Systems) in the presence or absence of 200 nM GP_{33} or NP_{396} peptide. In Supplemental Figure 3, splenocytes were incubated with or without NP_{396} peptide or with or without rIL-12 and IL-18, IL-12, and TNF-α, or IL-12 and IL-15 (R&D Systems).

In Figure 7, splenocytes were incubated with or without 50 μg/mL anti–IL-12 (C17.8), anti–IFN-γ (XM1.2), and anti–TNF-α (XT22) (all produced in the Harty laboratory at the University of Iowa) or a mix of all anti-cytokines in the presence of 200 nM NP_{396} peptide.

After incubation, surface staining was conducted by incubation of splenocytes with Ab cocktails for 20 minutes at 4°C. Endogenous ($Thy1.1^-$) and P14 or OT-I ($Thy1.1^+$) memory cells were distinguished from one another based on surface staining with anti-CD8 (clone 53-6.7, eBioscience) and anti-Thy1.1 (clone His51, eBioscience). In Figure 3, endogenous Ag-experienced $CD8^+$ T cells and P14 cells were detected based on surface staining with anti-Thy1.1 (clone His51, eBioscience), anti-CD8 (clone 53-6.7, eBioscience), and anti-CD11a (clone M17/4, eBioscience) as previously described (49). Cells were then permeabilized and stained intracellularly using anti–IFN-γ (clone XMG1.2, eBioscience). Flow cytometry data were acquired using FACSCanto (BD Biosciences) and analyzed using FlowJo software (Tree Star Inc.).

ICS for mouse samples after stimulation with in vitro peptide-pulsed or whole pathogens. Splenocytes from a naive C57BL/6 mouse were collected and processed into a single-cell suspension. Cells were CFSE-labeled by washing 3 times in PBS, incubation of 10^7 cells/mL in room-temperature PBS for 15 minutes in the presence of 5 mM CFSE, incubation on ice for 5 minutes with 1 mL of FCS, and washing 3 times with RPMI containing 10% FCS. Cells were resuspended in RPMI containing 10% FCS.

Cells were then plated at 5×10^6 cells per well; RPMI containing 10% FCS, 200-nM concentrations of GP_{33} or NP_{396} peptide, or 5×10^6 PFU of VacV-GP_{33}, VacV-OVA, or VacV-NP was added to wells; and plates were incubated for 18 hours at 37°C. After incubation, cells were washed twice with RPMI containing 10% FCS and resuspended at 5×10^6 cells/mL in RPMI containing 10% FCS.

Cells were plated at 5×10^4, 2.5×10^5, 5×10^5, or 2.5×10^6 cells per well along with 2×10^6 splenocytes from an LCMV-immune mouse, or from an LCMV-immune mouse that received adoptive transfer of P14 cells prior to infection. Cells were incubated for a total of 8 hours with BFA present during the entire incubation (0+8), for the final 6 hours of incubation (2+6), for the final 4 hours of incubation (4+4), or for the final hour of incubation (7+1).

After incubation, cells were surface-stained with anti-Thy1.1 (clone His51, eBioscience), anti-CD8 (clone 53-6.7, eBioscience), and anti-CD11a (clone M17/4, eBioscience). Cells were then permeabilized and stained intracellularly using anti–IFN-γ (clone XMG1.2, eBioscience). Data were acquired using FACSCanto (BD Biosciences) and analyzed using FlowJo software (Tree Star Inc.).

In Supplemental Figure 5, splenocytes from an LCMV-immune mouse containing P14 cells were mixed with CFSE-labeled splenocytes from an LM-OVA/B8R–immune mouse. Then 4×10^6 cells were plated and incubated for 12, 16, or 20 hours with 5×10^6 PFU of VacV-GP_{33} or 1×10^7 CFU of LM-OVA/B8R and with or without 50 μg/mL anti–IL-12, anti–IFN-γ, anti–TNF-α, or a mix of all anti-cytokines, and with BFA present for the final 4 hours of incubation.

Quantitative reverse transcriptase PCR. Spleens of mice containing memory P14 cells were collected, and tissue was processed into single-cell suspension. Cells were plated and incubated with 200 nM NP_{396} peptide for a total of 8 hours with BFA present for the entire incubation (0+8) or for the final hour of incubation (7+1). Cells were then surface-stained for CD8 and Thy1.1 and purified with anti-PE magnetic bead sorting (Miltenyi Biotec) using standard protocols. P14 cells were then sorted from purified cells using a BD FACSAria II flow cytometer (BD Biosciences). Total RNA was reverse-transcribed using a QuantiTech Reverse Transcription Kit (Qiagen), and cDNA was analyzed for expression of *Il12rb2*, *Ifngr1*, *Ifngr2*, and *Tnfrsf1b* by quantitative PCR using SYBR Advantage qPCR premix (Clontech) on an ABI 7300 Real Time PCR System (Applied Biosystems). Relative gene expression levels in each sample were normalized to that of a housekeeping gene, hypoxanthine phosphoribosyltransferase 1 (*Hprt1*).

Primers used were as follows: *Il12rb2*, 5′-GTGTCTGCAGCCAACTCAAA and 3′-AGGCTGCCAGGTCACTAGAA; *Ifngr1*, 5′-GCTGGGTCCACTCTGCAAAT and 3′-GGCTTTGAGTAGCTTTCAGTTCAA; *Ifngr2*, 5′-GTGCTCCAAACACCGTGAAC and 3′-GCCACGTTGCCAGTAATGAG; *Tnfrsf1b*, 5′-TTGGGGCCGACTTGTTAAGG and 3′-TGGCTGTAAAGGTGGGATGG.

Statistics. Statistical analyses were performed using GraphPad Prism software version 6 (GraphPad Software Inc.). Statistical comparisons of cytokine production by samples that were incubated in the presence of BFA for the entire incubation (0+8 or 0+20) compared with samples that were incubated with BFA for the final hour (7+1) or final 4 hours (16+4), or of mRNA expression of cytokine receptors for cells that were incubated in the presence of BFA for the entire incubation (0+8) compared with samples that were incubated with BFA for the final hour (7+1), were done using the paired 2-tailed Student's *t* test, and a *P* value of less than 0.05 was considered significant. Statistical comparisons of cytokine production by human samples that were incubated in the presence of peptide pools and in the presence or absence of anti-cytokines and with BFA present for the entire incubation or the final 4 hours of incubation were done using a nonparametric ANOVA with repeated measures (Freedman's test) with Dunn's post hoc test for multiple comparisons with respect to 0+20 samples, and a *P* value of less than 0.05 was considered significant.

Study approval. Human studies involving malaria-vaccinated subjects were approved by the National Institute of Allergy and Infectious Diseases Institutional Review Board as previously described (63). All patients gave written informed consent. For blood donations collected from human patients at the University of Iowa, PBMCs were obtained from anonymous donors at the DeGowin Blood Center at the University of Iowa, and no identifying information was collected from donors. Donors consented to allow blood cells not used for donation to be used for purposes of research. The consent process and documents for these donors have been approved by the IRB of the University of Iowa. All experiments involving animals were approved by the IACUC of the University of Iowa.

Author contributions

MDM, IJJ, ASI, QS, HHX, RAS, JTH, and VPB designed the research studies. MDM, IJJ, ML, QS, and ASI performed the research and analyzed the data. MDM, IJJ, ASI, QS, RAS, JTH, and VPB discussed the results and implications. MDM, ASI, JTH, RAS, and VPB wrote the paper.

Acknowledgments

The authors thank Christina Winborn for help with maintenance of mouse colonies, and Christina Winborn, Stacey Hartwig, and Lecia Epping for preparation of reagents used in this study. Human sample analyses were supported by the Intramural Research Program of the NIH. Some of the data presented herein were obtained at the Flow Cytometry Facility, which is a Carver College of Medicine/Holden Comprehensive Cancer Center core research facility at the University of Iowa. The facility is funded through user fees and the generous financial support of the Carver College of Medicine, Holden Comprehensive Cancer Center, and Iowa City Veterans Administration Medical Center. Research using the FACSAria was supported by the National Center for Research Resources of the NIH under Award 1 S10OD016199-01A1. This work was supported by NIH grants AI42767, AI85515, and AI100527 (to JTH), AI114543 (to JTH and VPB), GM113961 (to VPB), AI139874 (to HHX), and T32AI007485 and T32AI007511 (to IJJ), by Veteran Affairs BLR&D Merit Review Program BX002903A (to HHX), and by National Cancer Institute award 4T32AI007260-30 (Holden Comprehensive Cancer Center).

Address correspondence to: Vladimir Badovinac, University of Iowa, 3-550 Bowen Science Building, Iowa City, Iowa 52242, USA. Phone: 319.384.2930; Email: vladimir-badovinac@uiowa.edu. Or to: Robert A. Seder, Vaccine Research Center, National Institute of Allergy and Infectious Diseases, NIH, 40 Convent Drive, Building 40, Room 3512, Bethesda, Maryland 20814, USA. Phone: 301.594.8483; Email: rseder@mail.nih.gov.

1. Masopust D. Developing an HIV cytotoxic T-lymphocyte vaccine: issues of CD8 T-cell quantity, quality and location. *J Intern Med*. 2009;265(1):125–137.
2. Brown LE, Kelso A. Prospects for an influenza vaccine that induces cross-protective cytotoxic T lymphocytes. *Immunol Cell Biol*. 2009;87(4):300–308.
3. Thomas PG, Keating R, Hulse-Post DJ, Doherty PC. Cell-mediated protection in influenza infection. *Emerging Infect Dis*. 2006;12(1):48–54.
4. Epstein JE, et al. Live attenuated malaria vaccine designed to protect through hepatic CD8(+) T cell immunity. *Science*. 2011;334(6055):475–480.
5. Sahin U, et al. Personalized RNA mutanome vaccines mobilize poly-specific therapeutic immunity against cancer. *Nature*. 2017;547(7662):222–226.
6. Seder RA, et al. Protection against malaria by intravenous immunization with a nonreplicating sporozoite vaccine. *Science*. 2013;341(6152):1359–1365.
7. Schmidt NW, et al. Memory CD8 T cell responses exceeding a large but definable threshold provide long-term immunity to malaria. *Proc Natl Acad Sci U S A*. 2008;105(37):14017–14022.
8. Wolfl M, et al. Activation-induced expression of CD137 permits detection, isolation, and expansion of the full repertoire of $CD8^+$ T cells responding to antigen without requiring knowledge of epitope specificities. *Blood*. 2007;110(1):201–210.
9. Bansal A, et al. Enhanced recognition of HIV-1 cryptic epitopes restricted by HLA class I alleles associated with a favorable clinical outcome. *J Acquir Immune Defic Syndr*. 2015;70(1):1–8.
10. Chu H, George SL, Stinchcomb DT, Osorio JE, Partidos CD. $CD8^+$ T-cell responses in flavivirus-naive individuals following immunization with a live-attenuated tetravalent dengue vaccine candidate. *J Infect Dis*. 2015;212(10):1618–1628.
11. Smith KN, et al. Dendritic cells restore $CD8^+$ T cell reactivity to autologous HIV-1. *J Virol*. 2014;88(17):9976–9990.
12. Turtle L, et al. Human T cell responses to Japanese encephalitis virus in health and disease. *J Exp Med*. 2016;213(7):1331–1352.
13. Kutscher S, et al. Overnight resting of PBMC changes functional signatures of antigen specific T- cell responses: impact for immune monitoring within clinical trials. *PLoS One*. 2013;8(10):e76215.
14. Gold MC, et al. Human thymic MR1-restricted MAIT cells are innate pathogen-reactive effectors that adapt following thymic egress. *Mucosal Immunol*. 2013;6(1):35–44.
15. Fuchs YF, et al. Vagaries of the ELISpot assay: specific detection of antigen responsive cells requires purified CD8(+) T cells and MHC class I expressing antigen presenting cell lines. *Clin Immunol*. 2015;157(2):216–225.
16. Wipasa J, Wongkulab P, Chawansuntati K, Chaiwarit R, Supparatpinyo K. Cellular immune responses in HIV-negative immunodeficiency with anti-interferon-γ antibodies and opportunistic intracellular microorganisms. *PLoS One*. 2014;9(10):e110276.
17. Kelly C, et al. Chronic hepatitis C viral infection subverts vaccine-induced T-cell immunity in humans. *Hepatology*. 2016;63(5):1455–1470.
18. Riddell NE, et al. Multifunctional cytomegalovirus (CMV)-specific CD8(+) T cells are not restricted by telomere-related senescence in young or old adults. *Immunology*. 2015;144(4):549–560.
19. Bourguignon P, et al. Processing of blood samples influences PBMC viability and outcome of cell-mediated immune responses in antiretroviral therapy-naïve HIV-1-infected patients. *J Immunol Methods*. 2014;414:1–10.
20. Kløverpris HN, et al. Early antigen presentation of protective HIV-1 KF11Gag and KK10Gag epitopes from incoming viral particles facilitates rapid recognition of infected cells by specific $CD8^+$ T cells. *J Virol*. 2013;87(5):2628–2638.
21. Bacher P, et al. Antigen-reactive T cell enrichment for direct, high-resolution analysis of the human naive and memory Th cell repertoire. *J Immunol*. 2013;190(8):3967–3976.
22. Kagina BM, et al. Qualification of a whole blood intracellular cytokine staining assay to measure mycobacteria-specific CD4 and CD8 T cell immunity by flow cytometry. *J Immunol Methods*. 2015;417:22–33.
23. Singh SK, et al. The simultaneous ex vivo detection of low-frequency antigen-specific $CD4^+$ and $CD8^+$ T-cell responses using overlapping peptide pools. *Cancer Immunol Immunother*. 2012;61(11):1953–1963.
24. Mingozzi F, et al. AAV-1-mediated gene transfer to skeletal muscle in humans results in dose-dependent activation of capsid-specific T cells. *Blood*. 2009;114(10):2077–2086.
25. Rezvani K, et al. Leukemia-associated antigen-specific T-cell responses following combined PR1 and WT1 peptide vaccination in patients with myeloid malignancies. *Blood*. 2008;111(1):236–242.
26. Guihot A, et al. Multicentric Castleman disease is associated with polyfunctional effector memory HHV-8-specific $CD8^+$ T cells. *Blood*. 2008;111(3):1387–1395.

27. Rezvani K, et al. Graft-versus-leukemia effects associated with detectable Wilms tumor-1 specific T lymphocytes after allogeneic stem-cell transplantation for acute lymphoblastic leukemia. *Blood*. 2007;110(6):1924–1932.
28. Tae Yu H, et al. Characterization of CD8(+) CD57(+) T cells in patients with acute myocardial infarction. *Cell Mol Immunol*. 2015;12(4):466–473.
29. Spielmann G, Bollard CM, Kunz H, Hanley PJ, Simpson RJ. A single exercise bout enhances the manufacture of viral-specific T-cells from healthy donors: implications for allogeneic adoptive transfer immunotherapy. *Sci Rep*. 2016;6:25852.
30. Pulko V, et al. Human memory T cells with a naive phenotype accumulate with aging and respond to persistent viruses. *Nat Immunol*. 2016;17(8):966–975.
31. Rivino L, et al. Virus-specific T lymphocytes home to the skin during natural dengue infection. *Sci Transl Med*. 2015;7(278):278ra35.
32. Smaill F, et al. A human type 5 adenovirus-based tuberculosis vaccine induces robust T cell responses in humans despite preexisting anti-adenovirus immunity. *Sci Transl Med*. 2013;5(205):205ra134.
33. Swadling L, et al. A human vaccine strategy based on chimpanzee adenoviral and MVA vectors that primes, boosts, and sustains functional HCV-specific T cell memory. *Sci Transl Med*. 2014;6(261):261ra153.
34. Maldonado L, et al. Intramuscular therapeutic vaccination targeting HPV16 induces T cell responses that localize in mucosal lesions. *Sci Transl Med*. 2014;6(221):221ra13.
35. Green CA, et al. Chimpanzee adenovirus- and MVA-vectored respiratory syncytial virus vaccine is safe and immunogenic in adults. *Sci Transl Med*. 2015;7(300):300ra126.
36. Ogwang C, et al. Prime-boost vaccination with chimpanzee adenovirus and modified vaccinia Ankara encoding TRAP provides partial protection against Plasmodium falciparum infection in Kenyan adults. *Sci Transl Med*. 2015;7(286):286re5.
37. Ewer KJ, et al. Protective CD8$^+$ T-cell immunity to human malaria induced by chimpanzee adenovirus-MVA immunisation. *Nat Commun*. 2013;4:2836.
38. Barnes E, et al. Novel adenovirus-based vaccines induce broad and sustained T cell responses to HCV in man. *Sci Transl Med*. 2012;4(115):115ra1.
39. Bagarazzi ML, et al. Immunotherapy against HPV16/18 generates potent TH1 and cytotoxic cellular immune responses. *Sci Transl Med*. 2012;4(155):155ra138.
40. Berg RE, Cordes CJ, Forman J. Contribution of CD8$^+$ T cells to innate immunity: IFN-γ secretion induced by IL-12 and IL-18. *Eur J Immunol*. 2002;32(10):2807–2816.
41. Berg RE, Crossley E, Murray S, Forman J. Memory CD8$^+$ T cells provide innate immune protection against Listeria monocytogenes in the absence of cognate antigen. *J Exp Med*. 2003;198(10):1583–1593.
42. Freeman BE, Hammarlund E, Raué HP, Slifka MK. Regulation of innate CD8$^+$ T-cell activation mediated by cytokines. *Proc Natl Acad Sci U S A*. 2012;109(25):9971–9976.
43. Luke TC, Hoffman SL. Rationale and plans for developing a non-replicating, metabolically active, radiation-attenuated Plasmodium falciparum sporozoite vaccine. *J Exp Biol*. 2003;206(pt 21):3803–3808.
44. Brophy SE, Jones LL, Holler PD, Kranz DM. Cellular uptake followed by class I MHC presentation of some exogenous peptides contributes to T cell stimulatory capacity. *Mol Immunol*. 2007;44(9):2184–2194.
45. Homann D, Teyton L, Oldstone MB. Differential regulation of antiviral T-cell immunity results in stable CD8$^+$ but declining CD4$^+$ T-cell memory. *Nat Med*. 2001;7(8):913–919.
46. Martin MD, Shan Q, Xue HH, Badovinac VP. Time and antigen-stimulation history influence memory CD8 T cell bystander responses. *Front Immunol*. 2017;8:634.
47. Thome JJ, et al. Spatial map of human T cell compartmentalization and maintenance over decades of life. *Cell*. 2014;159(4):814–828.
48. Odumade OA, Knight JA, Schmeling DO, Masopust D, Balfour HH, Hogquist KA. Primary Epstein-Barr virus infection does not erode preexisting CD8(+) T cell memory in humans. *J Exp Med*. 2012;209(3):471–478.
49. Rai D, Pham NL, Harty JT, Badovinac VP. Tracking the total CD8 T cell response to infection reveals substantial discordance in magnitude and kinetics between inbred and outbred hosts. *J Immunol*. 2009;183(12):7672–7681.
50. Martin MD, Danahy DB, Hartwig SM, Harty JT, Badovinac VP. Revealing the complexity in CD8 T cell responses to infection in Inbred C57B/6 versus outbred Swiss mice. *Front Immunol*. 2017;8:1527.
51. Papadakis KA, et al. TL1A synergizes with IL-12 and IL-18 to enhance IFN-γ production in human T cells and NK cells. *J Immunol*. 2004;172(11):7002–7007.
52. Smeltz RB. Profound enhancement of the IL-12/IL-18 pathway of IFN-γ secretion in human CD8$^+$ memory T cell subsets via IL-15. *J Immunol*. 2007;178(8):4786–4792.
53. Bou Ghanem EN, D'Orazio SE. Human CD8$^+$ T cells display a differential ability to undergo cytokine-driven bystander activation. *Cell Immunol*. 2011;272(1):79–86.
54. Letimier FA, Passini N, Gasparian S, Bianchi E, Rogge L. Chromatin remodeling by the SWI/SNF-like BAF complex and STAT4 activation synergistically induce IL-12Rβ2 expression during human Th1 cell differentiation. *EMBO J*. 2007;26(5):1292–1302.
55. Li J, Yin Q, Wu H. Structural basis of signal transduction in the TNF receptor superfamily. *Adv Immunol*. 2013;119:135–153.
56. Platanias LC. Mechanisms of type-I- and type-II-interferon-mediated signalling. *Nat Rev Immunol*. 2005;5(5):375–386.
57. Bijker EM, et al. Cytotoxic markers associate with protection against malaria in human volunteers immunized with Plasmodium falciparum sporozoites. *J Infect Dis*. 2014;210(10):1605–1615.
58. Bastiaens GJH, et al. Safety, immunogenicity, and protective efficacy of intradermal immunization with aseptic, purified, cryopreserved Plasmodium falciparum sporozoites in volunteers under chloroquine prophylaxis: a randomized controlled trial. *Am J Trop Med Hyg*. 2016;94(3):663–673.
59. Van Braeckel-Budimir N, et al. A T cell receptor locus harbors a malaria-specific immune response gene. *Immunity*. 2017;47(5):835–847.e4.
60. Navarrete MA. ELISpot and DC-ELISpot assay to measure frequency of antigen-specific IFNγ-secreting cells. *Methods Mol Biol*. 2015;1318:79–86.
61. Altman JD, et al. Phenotypic analysis of antigen-specific T lymphocytes. *Science*. 1996;274(5284):94–96.
62. Nolz JC, Rai D, Badovinac VP, Harty JT. Division-linked generation of death-intermediates regulates the numerical stability of memory CD8 T cells. *Proc Natl Acad Sci U S A*. 2012;109(16):6199–6204.
63. Ishizuka AS, et al. Protection against malaria at 1 year and immune correlates following PfSPZ vaccination. *Nat Med*. 2016;22(6):614–623.
64. Hoffman SL, et al. Development of a metabolically active, non-replicating sporozoite vaccine to prevent Plasmodium falciparum malaria. *Hum Vaccin*. 2010;6(1):97–106.
65. Lyke KE, et al. Attenuated PfSPZ vaccine induces strain-transcending T cells and durable protection against heterologous controlled human malaria infection. *Proc Natl Acad Sci U S A*. 2017;114(10):2711–2716.